

Wide Field CCD Surface Photometry of the Giant Elliptical Galaxy NGC 4472 in the Virgo Cluster

Eunhyeuk Kim,¹ Myung Gyoon Lee,^{1*} and Doug Geisler²

¹*Department of Astronomy, Seoul National University, Seoul 151-742, Korea, Email: ekim@astro.snu.ac.kr, mglee@astrog.snu.ac.kr*

²*Departamento de Física, Universidad de Concepción, Casilla 160-C, Concepción, Chile, E-mail: doug@stars.cfm.udec.cl*

in original form 1999 April ??

ABSTRACT

We present deep wide field ($16'.4 \times 16'.4$) Washington CT_1 CCD surface photometry of the giant elliptical galaxy NGC 4472, the brightest member in the Virgo cluster. Our data cover a wider field than any previous CCD photometry as well as going deeper. Surface brightness profiles of NGC 4472 are not well fit by a single King model, but they can be fit approximately by two King models: with separate models for the inner and outer regions. Surface brightness profiles for the outer region can also be fit approximately by a deVaucouleurs law. There is clearly a negative color gradient within $3'$ of NGC 4472, in the sense that the color gets bluer with increasing radius. The slope of the color gradient for this region is derived to be $\Delta\mu(C - T_1) = -0.08 \text{ mag arcsec}^{-2}$ for $\Delta \log r = 1$, which corresponds to a metallicity gradient of $\Delta [\text{Fe}/\text{H}] = -0.2 \text{ dex}$. However, the surface color gets redder slowly with increasing radius beyond $3'$. A comparison of the structural parameters of NGC 4472 in C and T_1 images has shown that there is little difference in the ellipse shapes between isochromes and isophotes. In addition, photometric and structural parameters of NGC 4472 have been determined.

Key words: galaxies: NGC 4472 — galaxies: elliptical — galaxies: abundances — surface photometry — color gradient

1 INTRODUCTION

NGC 4472 (M49) is a giant elliptical galaxy in the Virgo cluster, located at 4° south of NGC 4486 (M87) at the center of the cluster. NGC 4472 is the brightest member of the Virgo cluster, some 0.2 mag brighter than the cD galaxy M87. NGC 4472 is an outstanding example of giant elliptical galaxies showing a bimodality in the color distribution of globular clusters (Geisler, Lee & Kim 1996; Lee, Kim & Geisler 1998). The bimodal color distribution of the globular clusters in NGC 4472 has shown that there are two kinds of cluster populations in this galaxy: a metal-poor population with a mean metallicity of $[\text{Fe}/\text{H}] = -1.3 \text{ dex}$ and a more spatially concentrated metal-rich population with a mean metallicity of $[\text{Fe}/\text{H}] = -0.1 \text{ dex}$. Interestingly it is found that the metal-rich globular clusters show some properties in common with the galaxy halo stars in their spatial distribution and color profiles, while the metal-poor globular clusters do not show such behavior. This result indicates that there may exist some connection between the metal-rich globular clusters and halo stars in NGC 4472 (Lee et al. 1998).

NGC 4472 is an ideal target to investigate the spatial distribution of stellar light as well as the properties of globular clusters in giant elliptical galaxies, because it is relatively nearby and is the brightest galaxy in the Virgo cluster. Information on the spatial distribution of galaxy light is very useful for understanding the structure and evolution of galaxies, and it provides important constraints for modeling galaxy formation.

To date there have been many surface photometry studies of NGC 4472, as summarized in Table 1. However, there is a large discrepancy in the photometry of the outer region of NGC 4472 among them, the details of which will be shown later. This large difference leads to different conclusions about the properties of NGC 4472. For example, Mihalas & Binney (1981) showed that the surface brightness profile of NGC 4472 given by King (1978) is beautifully fit by a King model with a concentration parameter ($c = 2.35$), while the surface brightness profile of this galaxy published later by Caon et al. (1994) is much flatter than that of King's in the outer region. McLaughlin (1999) pointed out this significant difference, and he adopted the data given by Caon et al. for the comparison of the halo stellar light and the globular clusters in NGC 4472. He described that the surface brightness profile of NGC 4472 is similar to the

* corresponding author, E-mail:mglee@astrog.snu.ac.kr

Table 1. Previous surface photometry of NGC 4472.

Author	Filter	Radial Coverage	Detector
King (1978)	<i>B</i>	1000''	photographic plate
Michard (1985)	<i>B</i>	560''	photographic plate
Lauer (1985)	<i>R</i>	33''	CCD
Cohen (1986)	<i>vgri</i>	400''	CCD
Boroson & Thompson (1987)	<i>Bri</i>	100''	CCD
Bender & Möllenhoff (1987)	<i>VRI</i>	73''	CCD
Peletier (1990)	<i>UBR</i>	180''	CCD
Caon et al. (1994)	<i>B</i>	1300''	photographic plate CCD for the inner 2'.4 × 4'.0 region
Ferrarese et al. (1994)	F555W	15''	CCD (HST PC)
This study	<i>CT</i> ₁	530''	CCD

surface number density profile of globular clusters in NGC 4472, which is contrary to the case of M87, as seen in his Fig. 3. If the surface photometry given by King were used instead, this conclusion no longer remains valid. To resolve this discrepancy requires good wide field surface photometry of NGC 4472. Until now, the combined requirements of accurate photometry over a wide field were difficult to meet in a single study, given the photometric limitations of photographic plates and the small size of CCDs.

In this paper we present wide field surface photometry of NGC 4472 based on deep CCD images taken with Washington *CT*₁ filters. This paper is organized as follows: In Section 2 observations and data reduction are described. Section 3 presents the results and Section 4 compares the results of this study with those of previous studies. Section 5 discusses the surface brightness profile and the color gradient. Finally the primary results are summarized in Section 6.

2 OBSERVATIONS AND DATA REDUCTION

Washington *CT*₁ CCD images of NGC 4472 were obtained at the prime focus of KPNO 4m telescope on the photometric night of 1993 February 26, with the primary purpose of studying the globular clusters in NGC 4472. We used Washington *CT*₁ filter system which is very efficient for measuring the metallicity of extragalactic globular clusters. The effective central wavelengths and bandpasses of *C* and *T*₁ filters are $\lambda_c = 3910\text{\AA}$, $\Delta\lambda = 1100\text{\AA}$, and $\lambda_c = 6330\text{\AA}$, $\Delta\lambda = 800\text{\AA}$, respectively (Canterna 1976). The size of the field is 16'.4 × 16'.4. The pixel scale of the CCD is 0.48 arcsec. We took 60s and 3 × 1000s *T*₁ exposures (short and long exposures, respectively, hereafter), and 5 × 1000s *C* exposures. The seeing was 1.25 arcsec. The images of the central region with $r < 8''$ of NGC 4472 in the *C* images were saturated so that we could not derive the colors for the central region. The details of the observations and transformation of the photometry to the standard system were described in Geisler et al. (1996).

Fig.1 displays a greyscale map of the short *T*₁ exposure image of NGC 4472, overlaid with isophotes. Fig. 1 shows that the inner region of NGC 4472 is less elliptical than the outer region. Surface photometry of NGC 4472 was obtained using the ellipse fitting software ELLIPSE in STS-

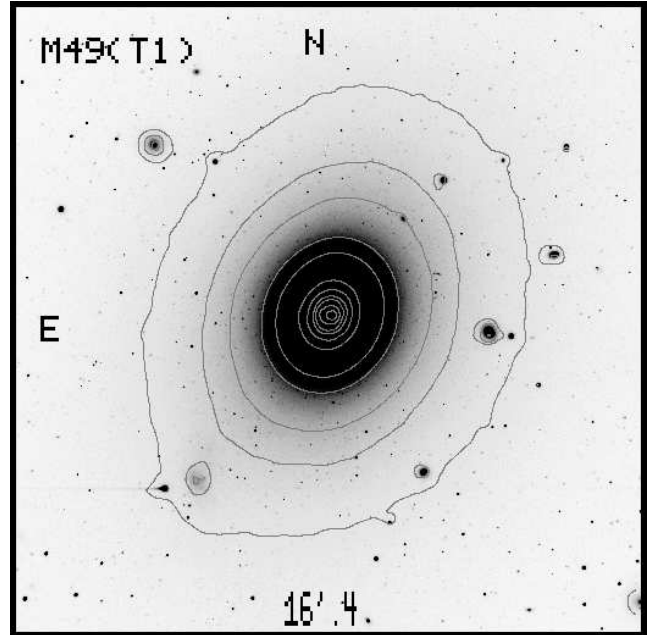


Figure 1. A greyscale map of the short *T*₁ exposure CCD image of NGC 4472, overlaid with isophotal contours. North is at the top, and east is to the left. The contour levels are $\mu(T_1) = 23.5, 22.6, 22.2, 21.4, 20.9, 19.9, 19.4, 19.0, 18.6, 18.1,$ and $17.6 \text{ mag arcsec}^{-2}$, respectively.

DAS/IRAF*, and polygonal aperture photometry software POLYPHOT in APPHOT/IRAF, independently. Comparison of the resulting surface photometries showed an excellent agreement within the errors between the two methods. We adopt the results obtained using ELLIPSE for the final analysis.

We have determined the sky background brightness from the clear region at the north-east corner of the image (the distance along the minor axis from the center of NGC 4472 is 10'.5), obtaining $\sim 20.80 \pm 0.02 \text{ mag arcsec}^{-2}$ for *T*₁ and $\sim 22.23 \pm 0.02 \text{ mag arcsec}^{-2}$ for *C*, respectively. These results correspond to $V = 21.22 \text{ mag arcsec}^{-2}$ and

* IRAF is distributed by the National Optical Astronomical Observatories, which is operated by the Association of Universities for Research in Astronomy, Inc., under cooperative agreement with the National Science Foundation.

$B = 22.09 \text{ mag arcsec}^{-2}$, respectively. The night sky brightness at the zenith measured at the Kitt Peak National Observatory under new moon is known to be $V = 21.91$ and $B = 22.91 \text{ mag arcsec}^{-2}$ (Pilachowski et al. 1989). Considering that the lunar phase when our data were obtained is 5 days from new moon (leading to a difference in the night sky brightness of $\Delta B = 0.7$ and $\Delta V = 0.2 \text{ mag arcsec}^{-2}$ (Elias 1994)) and that the air mass of our target is 1.1–1.4, our sky estimates are approximately consistent with the night sky brightness. This result shows that our sky measurement is reasonable for the surface photometry of the galaxy. We have estimated the contribution from the galaxy light at the radius for the sky measurement as follows. Using the de Vaucouleurs law, we have fit the surface brightness profile for the inner region of the galaxy where the surface photometry is affected little by the uncertainty in the sky value, and calculated the expected sky brightness at the position of the sky region, obtaining $T_1 \approx 26.50 \pm 0.33 \text{ mag arcsec}^{-2}$. This value is only 0.5 % of the sky brightness. Therefore any contribution from the galaxy light at the sky position is estimated to be negligible. The flat-fielding is accurate with an error smaller than one percent. So that a sky level measured near one corner of the chip can be applied to the whole area without introducing any significant error for the surface photometry of NGC 4472.

Since we have short and long T_1 exposure images, we can check the accuracy of our surface photometry by comparison. Fig. 2 displays the comparison of the T_1 surface brightness between the short and long exposure images. Fig. 2 shows good agreement between the two results: the differences in the surface brightness of the two exposures are on average smaller than $0.03 \text{ mag arcsec}^{-2}$ over the region with $r < 420''$, but get as large as $\sim 0.1 \text{ mag arcsec}^{-2}$ beyond $r = 420''$. Final data of the surface photometry were prepared by combining the long exposure data for $r > 3'$ and the average of the short and long exposure data for $r < 3'$, after matching the zero points in the brightness of the two. Table 2 lists the final surface photometry of NGC 4472 including the surface brightness, color, ellipticity and position angle as a function of the major axis. Preliminary results of this study were used for the comparison of halo light and globular clusters in NGC 4472 in Lee et al. (1998).

3 RESULTS

3.1 Surface Brightness Profiles

Radial surface brightness profiles of NGC 4472 are displayed in Fig. 3(a). The T_1 surface brightness covers a full 8.7 magnitude range. The shapes of the C and T_1 profiles are very similar in general. The shapes of the surface brightness profiles of NGC 4472 are typical for giant elliptical galaxies: flattening in the core region and falling off smoothly with increasing radius.

3.2 Surface Color Profiles

Fig. 3(b) displays the radial surface ($C - T_1$) color profile of NGC 4472. Here the surface color means the differential color per square-arcsecond. The surface colors for the central region with $r < 8''$ were not obtained, because of the

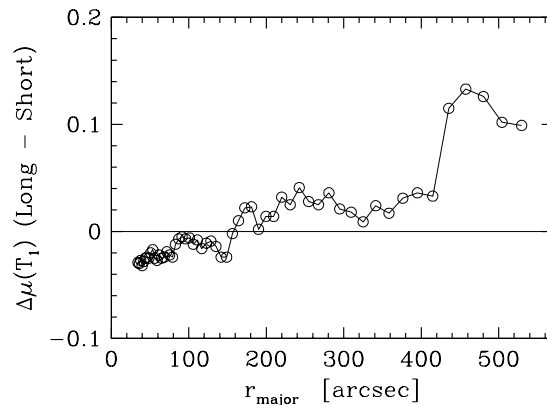


Figure 2. Comparison of the surface photometry between the long and short T_1 exposures. The difference is defined by the surface magnitude of the long exposure minus that of the short exposure.

saturation in the C image. Fig. 3(b) shows that there exists clearly a radial color gradient in NGC 4472. The surface color gets bluer as the radius increases until $r \sim 3'$. This feature is often seen in other giant elliptical galaxies (Cohen 1986; Kormendy & Djorgovski 1989; Peletier et al. 1990). However, the surface color gets slowly redder with increasing radius for the region with $3' < r < 7'.3$, and gets much redder with increasing radius beyond $r = 7'.3$. The outer region suffers more from the photometric errors than the inner region as shown by the error bars in the figure, but the reversal of the color gradient at $r \sim 3'$ appears to be real.

The mean color gradient for $r < 3'$ is measured to be $\Delta\mu(C - T_1) = -0.08 \text{ mag arcsec}^{-2}$ for $\Delta \log r = 1$, from the weighted linear least square fitting. We have transformed the ($C - T_1$) color gradient into the metallicity gradient using the relation given by Geisler & Forte (1990): $[\text{Fe}/\text{H}] = 2.35(C - T_1) - 4.39$, assuming the color gradient is entirely due to the metallicity gradient (Peletier et al. 1990). The resulting metallicity gradient of $\Delta [\text{Fe}/\text{H}] = -0.2 \text{ dex}$. This value is similar to a mean value of the metallicity gradients derived from the color gradients for giant elliptical galaxies (Peletier et al. 1990). The color profile for $r < 3'$ appears to consist of two linear components breaking at $\sim 30''$, the slopes of which are derived to be -0.046 and $-0.111 \text{ mag arcsec}^{-2}$, respectively. The color gradient for the outer region with $3' < r < 9'$ is measured to be $\Delta\mu(C - T_1) = +0.199$ for $\Delta \log r = 1$. If the fit is limited to $r < 7'.3$, the slope will be slightly reduced to 0.181.

3.3 Ellipticities and Position Angles

Radial profiles of ellipticity and position angle of NGC 4472 are presented in Figs. 4(a) and 4(b), respectively. Fig. 4 shows several features as follows. First, both C and T_1 profiles of ellipticity and position angle are almost the same over the entire range of radius measured in this study. This is again confirmed in the C and T_1 isophotal contour map of the fitted ellipses in Fig. 5. Fig. 5 shows that there is little difference in the shape and orientation of the C and T_1 isophotal contours of the fitted ellipses. This result shows

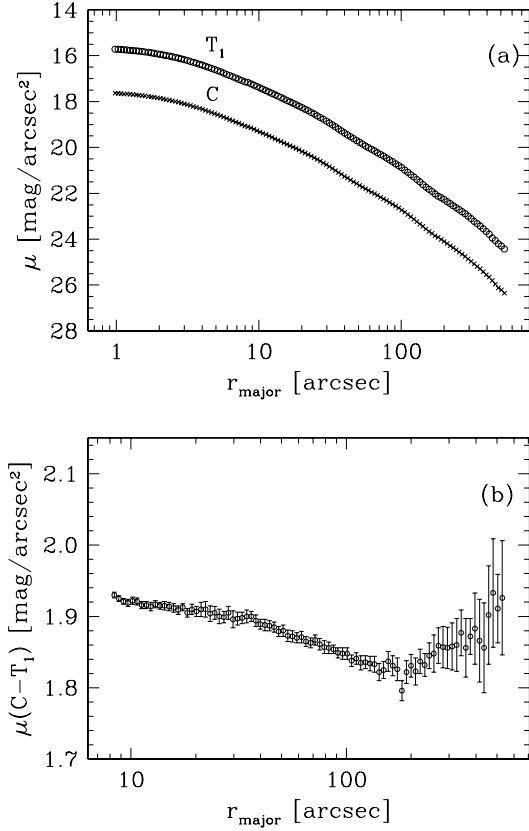


Figure 3. (a) Radial profiles of the surface brightness in T_1 (open circles) and C (crosses). (b) Radial variations of the surface $(C - T_1)$ color.

clearly that the shapes of the isophotes and isochromes of NGC 4472 are almost identical, which is consistent with previous findings based on the data of much smaller area than ours (Cohen 1986; Peletier et al. 1990). Secondly, the ellipticity decreases slightly from 0.1 at $r = 1''$ to 0.07 at $r \approx 4''$, and increases with increasing radius to ~ 0.18 at $r = 20''$. For the region at $20'' < r < 130''$ the ellipticity remains at ~ 0.2 with small fluctuations. Beyond this region the ellipticity continues to increase to 0.22 at the outer limit. Thus the inner region of NGC 4472 is more circular than the outer region. Thirdly, the position angle decreases rapidly from ~ 172 degrees at $r = 1''$ to 158 degrees at $r \approx 5''$, then decreases slowly to 153 degrees with increasing radius at the outer region, showing that the isophotes of NGC 4472 rotate almost 20 degrees with increasing radius.

We have compared the radial profiles of the ellipticity and position angle for the central region at $r < 15''$ with those based on the HST observations by van den Bosch et al. (1994). The comparison, included in Figure 4, shows that the two results are in good agreement. Rapid changes of the ellipticity and position angle in the inner $r < 2''$ are probably caused by the presence of dust which is visible at $0''.3 < r < 1''.5$ at position angle 140° (Jaffe et al. 1994).

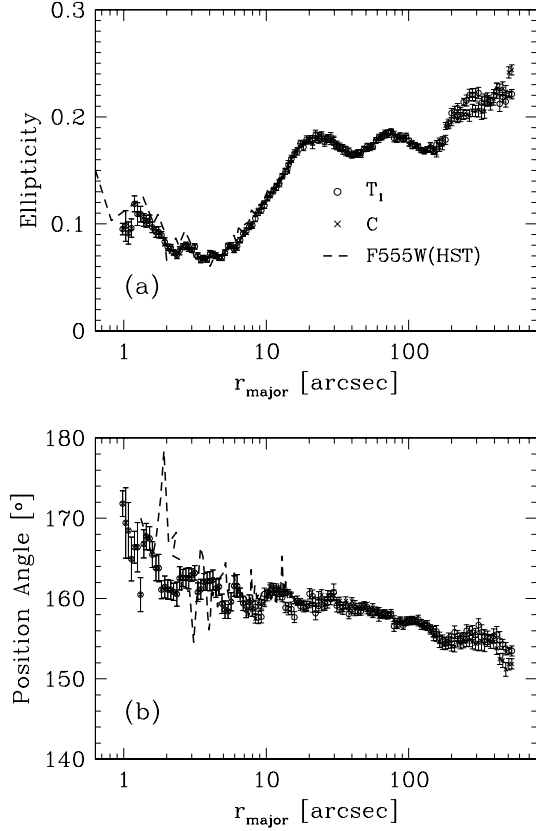


Figure 4. (a) Radial profiles of the ellipticities in C and T_1 . The symbols are the same as in Fig. 3(a). (b) Radial profiles of the position angles.

3.4 Total Magnitude, Total Color and the Size of NGC 4472

We have calculated the total magnitude and color of NGC 4472 by integrating the radial surface brightness profiles out to the limiting radius, obtaining $T_1(\text{total}) = 7.76 \pm 0.02$ mag and $(C - T_1)(\text{total}) = 1.87 \pm 0.03$ mag, respectively. We have transformed these results into B magnitude and $(B - V)$ color using the relations given by Geisler (1996). The transformed magnitude and color ($B_T = 9.26$ mag, $(B - V)_T = 0.92$) are in excellent agreement with those in de Vaucouleurs et al. (1991), $B_T = 9.25$ mag, and $(B - V)_T = 0.95$. However, our magnitude is ~ 0.4 mag fainter than that given by Caon et al. (1994). Lee et al. (1998) used the total magnitude of NGC 4472 given by de Vaucouleurs et al. (1991) which agrees well with ours, for calculating the specific frequency of the globular clusters in NGC 4472. Therefore the results on the specific frequency of the globular clusters in NGC 4472 given by Lee et al. (1998) remain valid.

The integrated $(C - T_1)$ color (within given radius) gets bluer with increasing radius out to $r \simeq 3'$. Beyond this radius, the integrated color remains at $(C - T_1) \simeq 1.87$. The surface color gets slowly redder outward for $r > 3'$, but the surface brightness is so low in the outer region that the integrated color change little with increasing radius.

We have also derived a standard radius of NGC 4472,

Table 2. Surface photometry of NGC 4472.

r_{major} (arcsec)	$\mu(T_1)$	$\mu(C - T_1)$	Ellipticity(T_1)	Position Angle ($^\circ$) (T_1)
0.98	15.714 ± 0.001	—	0.095 ± 0.005	171.84 ± 1.60
1.59	15.834 ± 0.001	—	0.097 ± 0.005	165.47 ± 1.61
2.60	16.076 ± 0.002	—	0.079 ± 0.003	162.57 ± 1.05
4.23	16.461 ± 0.003	—	0.071 ± 0.003	162.32 ± 1.25
6.24	16.869 ± 0.004	—	0.080 ± 0.004	161.58 ± 1.42
8.37	17.166 ± 0.004	1.930 ± 0.004	0.105 ± 0.003	158.96 ± 0.86
10.18	17.401 ± 0.004	1.922 ± 0.005	0.124 ± 0.003	160.35 ± 0.65
12.37	17.647 ± 0.005	1.914 ± 0.006	0.138 ± 0.003	160.57 ± 0.73
15.03	17.887 ± 0.005	1.914 ± 0.006	0.161 ± 0.003	158.69 ± 0.64
18.27	18.137 ± 0.005	1.905 ± 0.006	0.172 ± 0.004	158.97 ± 0.64
22.21	18.400 ± 0.008	1.910 ± 0.011	0.183 ± 0.005	158.18 ± 0.84
27.00	18.695 ± 0.006	1.899 ± 0.008	0.180 ± 0.004	159.49 ± 0.65
32.82	19.019 ± 0.007	1.898 ± 0.008	0.172 ± 0.004	158.91 ± 0.69
39.89	19.368 ± 0.006	1.889 ± 0.007	0.164 ± 0.003	158.62 ± 0.51
48.48	19.697 ± 0.005	1.879 ± 0.007	0.170 ± 0.003	159.12 ± 0.47
58.93	20.006 ± 0.006	1.870 ± 0.007	0.178 ± 0.003	158.48 ± 0.49
71.64	20.302 ± 0.006	1.867 ± 0.007	0.185 ± 0.003	157.94 ± 0.49
87.08	20.622 ± 0.005	1.854 ± 0.006	0.183 ± 0.002	157.30 ± 0.44
105.84	20.985 ± 0.007	1.838 ± 0.008	0.173 ± 0.003	157.33 ± 0.47
128.65	21.399 ± 0.009	1.834 ± 0.010	0.168 ± 0.003	156.72 ± 0.50
156.37	21.824 ± 0.012	1.837 ± 0.014	0.174 ± 0.004	155.93 ± 0.70
190.08	22.188 ± 0.014	1.822 ± 0.016	0.194 ± 0.004	155.03 ± 0.68
231.03	22.541 ± 0.013	1.832 ± 0.016	0.205 ± 0.004	155.06 ± 0.67
280.82	22.891 ± 0.026	1.857 ± 0.029	0.221 ± 0.006	155.78 ± 0.85
341.34	23.315 ± 0.025	1.877 ± 0.032	0.216 ± 0.005	155.33 ± 0.79
414.91	23.788 ± 0.054	1.866 ± 0.058	0.224 ± 0.007	155.53 ± 1.01
504.32	24.302 ± 0.039	1.911 ± 0.048	0.221 ± 0.003	153.49 ± 0.41
529.54	24.432 ± 0.076	1.926 ± 0.080	0.221 ± 0.004	153.49 ± 0.63

which is defined as the radius where the surface brightness in B band is $25 \text{ mag arcsec}^{-2}$: $r_{25} \simeq 313''$, which corresponds to a linear size of 51.7 kpc for the adopted distance of 17.4 Mpc (Lee, Kim & Geisler 1998). This value is a little smaller than the result of Caon et al. (1990), $350''$. In Table 3 we have summarized the photometric parameters of NGC 4472 derived in this study.

4 COMPARISON WITH PREVIOUS STUDIES

We have compared our results with those given by previous studies which are listed in Table 1. While previous photographic studies cover a wide field of NGC 4472, previous CCD studies are limited to a small field except for the study by Cohen (1986) which covers up to $r \sim 400''$. Previous surface photometry of NGC 4472 was presented in various photometric systems. For the comparison we transformed approximately the results of surface photometry in different filters into the BVR system, using the conversion relations given in the literature which are listed in Table 4.

4.1 Surface Brightness Profiles

Fig. 6 displays the comparison of the surface brightness profiles between this study and others, plotting the differences between our value and theirs. The surface brightness profiles of this study and others agree roughly for the inner region at $r < 100''$, except for the B profile given by Boroson & Thompson (1987) which is about 0.4 mag brighter than the others. In particular, the profiles of this study and Peletier et

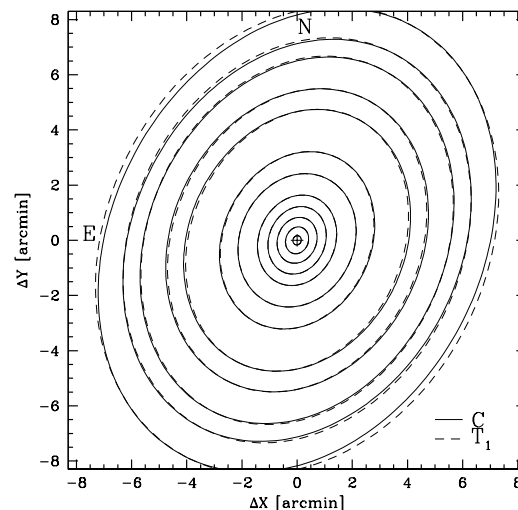


Figure 5. Ellipses fitted to the isophotes of C (solid lines) and T_1 (dotted lines) images. The major radii of the ellipses are 10, 30, 50, 75, 100, 148, 199, 294, 341, 414, 457, and 530 arcsec.

al. (1990) show an excellent agreement for $r < 100''$. However, the differences among these results become significant for the outer region at $r > 100''$. For $r > 100''$ the surface brightness profile given by Caon et al. becomes fainter

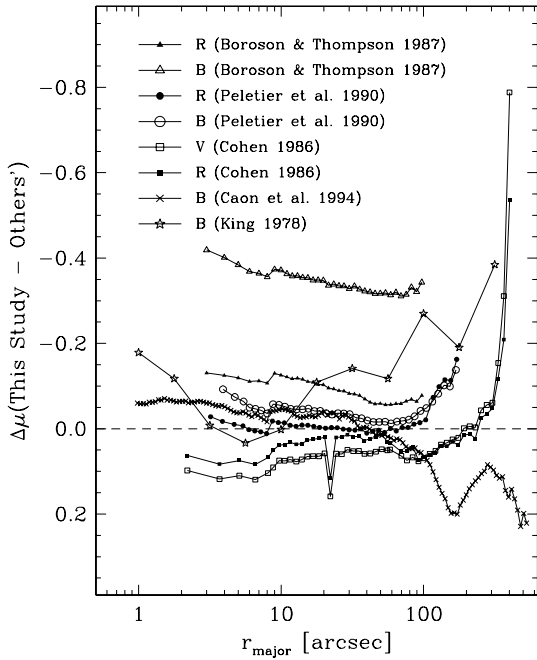


Figure 6. Comparison of the surface brightness of NGC 4472 between this study and other studies.

than ours, while those of the others become brighter than ours. Note the two photographic results by King (1978) and Caon et al. (1994) show opposite trends to each other for the outer region, and that our photometry stays between the two. The large differences in the surface brightness profiles for the outer region are probably due to the difficulty in estimating sky values in images, as well as the larger photometric errors from the diminishing galaxy light.

4.2 Surface Color Profiles

Fig. 7 displays the comparison of the surface color profiles of NGC 4472 obtained in this study and others. It is seen that for the inner region at $r < 100''$ ($U - R$), ($C - T_1$), ($V - I$), ($B - R$), and ($v - g$) colors show obviously negative radial gradients, while ($r - i$) and ($g - r$) show positive radial gradients. For the very outer region, ($g - r$) and ($g - i$) colors change much more significantly than does ($C - T_1$). This appears to be due to large errors in the ($g - r$) and ($g - i$) colors, as seen in Fig. 6.

5 DISCUSSION

5.1 The Shape of the Surface Brightness Profiles

In Fig. 8 we have fit the surface brightness profiles of NGC 4472 using King models and de Vaucouleurs law. Fig. 8 displays the T_1 surface brightness profile of NGC 4472 obtained in this study and the surface brightness of the central region at $r < 15''$ based on the HST observation by Ferrarese et al. (1994). We have transformed the V surface photometry

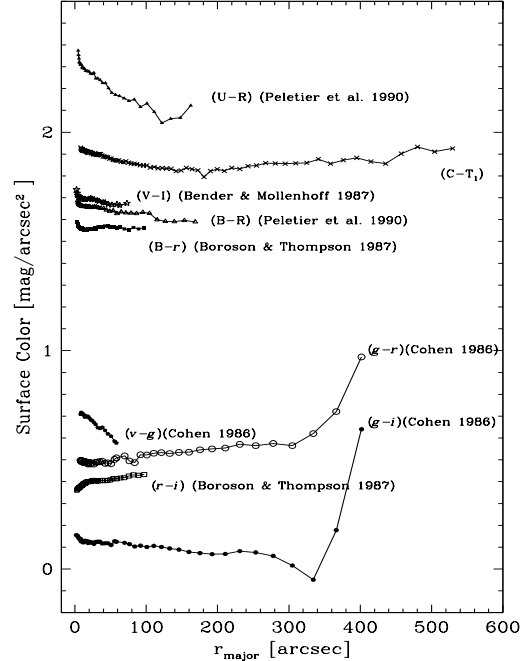


Figure 7. Comparison of the color profiles of NGC 4472 between this study and other studies.

of the central region into the T_1 magnitude using the conversion relation given by Geisler (1996). Here the surface brightness profile is plotted against the geometric mean of the major and minor radii ($r = \sqrt{(r_{\text{major}} * r_{\text{minor}})}$). Fig. 8 shows that both photometry sets are in excellent agreement.

In Fig. 8(a) it is found that the entire surface brightness profile cannot be fit by any single King model, but it can be fit approximately by two King models. The outer region at $r > 10''$ is approximately fit by a King model with a concentration parameter $c = (\log r_t/r_c) = 2.35$ and $r_c = 5''$ ($= 420$ pc), while the inner region at $r < 7''$ is fit well by a King model with $c = 2.50$ and $r_c = 4''$ ($= 340$ pc) (where r_t and r_c represent, respectively, tidal radius and core radius). Ferrarese et al. (1994) also pointed out that the surface brightness profile of the central region ($r < 15''$) could not be fit by any single King model.

The surface brightness profile of the outer region $r > 7''$ of NGC 4472 is also fit approximately by a deVaucouleurs law, as shown in Figs. 8(a) and 8(b), while that of the inner region is far from being fit by a deVaucouleurs law. The solid line in Fig. 8 represents a fit to the data for $7'' < r < 260''$, $\mu(T_1) = 2.52(\pm 0.07)r^{1/4} + 13.09$ with $\sigma = 0.08$. The corresponding effective radius is derived to be $r_e = 120 \pm 2$ arcsec, ($= 10.1$ kpc).

The evidence found in this study clearly indicates that there is a distinct component in the central region of NGC 4472: the presence of two components in the surface brightness profile, the reversal of the ellipticity profile, and the rapid change in the profile of the position angle in the inner region at $r < 4''$. Interestingly it is known that NGC 4472 has a kinematically decoupled core and shows enhanced Mg₂ in the inner $5''$ (Davis & Birkinshaw 1988; Ferrarese et al.

Table 3. Photometric parameters of NGC 4472.

Parameter	Symbol	Value	Reference ^a
Core radius of the nucleus	r_c	3.6'', 300 pc	1
Standard radius	r_{25}	313'', 51.7 kpc	1
Effective radius	$r_e(T_1)$	120'', 10.1 kpc	1
Effective surface brightness	$\mu_e(T_1)$	21.40 ± 0.03	1
Effective surface color	$\mu_e(C - T_1)$	1.83 ± 0.04	1
Ellipticity at $r_e(T_1)$	$\epsilon_e(T_1)$	0.175 ± 0.004	1
Position angle at $r_e(T_1)$	$PA_e(T_1)$	$155^\circ.4 \pm 0^\circ.7$	1
Mean ellipticity	$\langle \epsilon \rangle$	0.186 ± 0.016	1
Mean position angle	$\langle PA \rangle$	$155^\circ.1 \pm 0^\circ.6$	1
Ellipticity at r_{25}	ϵ_{25}	0.200 ± 0.006	1
Position angle at r_{25}	PA_{25}	$154^\circ.6 \pm 0^\circ.8$	1
Foreground reddening	$E(B - V)$	0.00	2
Distance modulus	$(m - M)_0$	31.2 ± 0.2	3
Distance	d	17.4 Mpc	3
Central surface brightness	$\mu_0(T_1)$	15.64 ± 0.03	1
Total magnitude	$T_1(\text{total})$	7.76 ± 0.02 mag	1
Total color	$(C - T_1)(\text{total})$	1.87 ± 0.03 mag	1
Absolute total magnitude	$M(T_1)$	-23.44 mag	1,3
Color gradient	$\Delta\mu(C - T_1)/(\Delta \log r = 1)$	$(r < 3')$ -0.08 mag arcsec ⁻² $(3' < r < 9')$ +0.20 mag arcsec ⁻²	1 1
Metallicity gradient	$\Delta[\text{Fe}/\text{H}]/(\Delta \log r = 1)$	$(r < 3')$ -0.2 dex $(3' < r < 9')$ +0.5 dex	1 1

^a References: (1) This study; (2) deVaucouleurs et al. 1991; (3) Lee, Kim & Geisler 1998.

Table 4. Conversion relations used for the comparison of the photometry of NGC 4472.

Relation	Reference
$B = 1.011C - 0.328(C - T_1) + 0.089$	Geisler 1996
$V = T_1 + 0.256(C - T_1) + 0.052$	Geisler 1996
$V = g - 0.42(g - r) - 0.03$	Kent 1985
$R = T_1 - 0.017(C - T_1) + 0.003$	Geisler 1996
$R = r - 0.039(r - i) - 0.293$	Barsony 1989
$(C - T_1) = 2.032(g - r) + 1.006$	Taylor 1985, Geisler 1996
$(B - R) = 0.748(C - T_1) + 0.125$	Geisler 1996

1989; Davies, Sadler & Peletier 1993). Therefore it is suspected that the central component may be related with the kinematically decoupled core, although van den Bosch et al. (1994) pointed out that the isophotal profiles show no evidence for a photometrically distinct nucleus.

5.2 Color Gradient

It is found that there is clearly a negative color gradient for $r < 3'$ ($= 15$ kpc) in NGC 4472 in the sense that the color gets bluer with increasing radius: $\Delta\mu(C - T_1) = -0.08$ mag arcsec⁻² for $\Delta \log r = 1$. In general, color gradients in giant elliptical galaxies are interpreted as evidence for a metallicity gradient, while color gradients in dwarf galaxies may be due to age effects (Vader et al. 1988; Peletier et al. 1990). The color gradient in the inner region of NGC 4472 corresponds to a metallicity gradient of $\Delta[\text{Fe}/\text{H}] = -0.2$ dex. This result is similar to that derived from the line-strength gradient for $3'' < r < 50''$ of NGC 4472 by Davies et al. (1993). This value for NGC 4472 is similar to the mean value known for giant elliptical galaxies, $\Delta[\text{Fe}/\text{H}] = -0.2 \pm 0.1$ dex (Kormendy & Djorgovski 1989; Peletier et al. 1990; Davies, Sadler & Peletier 1993).

The metallicity gradient in NGC 4472 may result from dissipational collapse. However, the metallicity gradients predicted by conventional models of galaxy formation based on dissipational collapse (Larson 1975; Carlberg 1984) are much steeper than the value observed in NGC 4472. Considering that the metallicity gradients can be diluted by a factor of 2 over three merger events (White 1980), Davies et al. (1993) pointed out that the shallow metallicity gradients support the hypothesis that giant elliptical galaxies form by stellar mergers, and that the line-strength (metallicity) gradient may be due to their progenitors which formed predominantly by dissipational collapse. Some of the observed properties of the globular clusters in NGC 4472 also support the merger hypothesis for the formation of NGC 4472, while some do not. This point was discussed in detail by Lee et al. (1998).

On the other hand, it is difficult to understand in terms of galaxy formation that the color profile of NGC 4472 shows a positive gradient in the outer region at $r > 3'$. This trend was also shown by the $(g - r)$ color profile given by Cohen (1986), but this $(g - r)$ color profile showed a positive color gradient even for the inner region which is contrary to others, as seen in Fig. 7. Other deep photometry of the outer region of NGC 4472 and other giant elliptical galaxies are needed to investigate this feature further.

6 SUMMARY AND CONCLUSIONS

We have presented surface photometry in Washington C and T_1 filters for a wide field centered on the brightest elliptical galaxy in Virgo, NGC 4472. Our data cover a wider field than those of any previous CCD surface photometry, and our photometry goes deeper than any previous photometry.

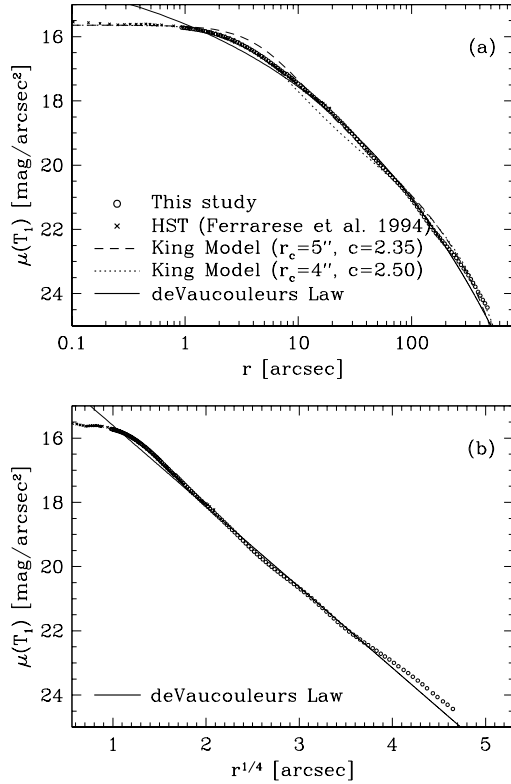


Figure 8. (a) Comparison of the surface brightness profiles of NGC 4472 (open circles) and King models with the concentration parameters $c = 2.35$ (the short dashed line) and $c = 2.50$ (the dotted line). The crosses represent the data based on the HST observations of the inner $15''$ region of NGC 4472 by Ferrarese et al. (1994). The solid line represents a profile of the deVaucouleurs law. (b) Comparison of the surface brightness profiles of NGC 4472 and deVaucouleurs law (the solid line).

Primary results obtained in this study are summarized as follows:

(1) Surface brightness profiles for the outer region of NGC 4472 obtained in this study lie between those found in the wide field photographic studies of King (1978) and Caon et al. (1994). The surface brightness profiles of NGC 4472 are not fit well by a single King model, but they can be fit approximately by two King models: one for the inner region and the other for the outer region. Surface brightness profiles for the outer region can be fit approximately also by a deVaucouleurs law.

(2) There is obviously a negative color gradient for the region at $r < 3'$ of NGC 4472 in the sense that the colors get bluer with increasing radius. The slope of the color gradient for this region is derived to be $\Delta\mu(C - T_1) = -0.08 \text{ mag arcsec}^{-2}$ for $\Delta \log r = 1$, which corresponds to a metallicity gradient of $\Delta[\text{Fe}/\text{H}] = -0.2 \text{ dex}$. However, the surface color appears to get redder slowly with increasing radius for the region with $r > 3'$.

(3) A comparison of the structural parameters of NGC 4472 in C and T_1 images has shown that there is little difference in the ellipse shapes between isochromes and isophotes.

(4) Photometric and structural parameters of NGC 4472 have been determined, which are listed in Table 3.

ACKNOWLEDGMENTS

This research is supported by the Ministry of Education, Basic Science Research Institute grant No.BSRI-98-5411 (to M.G.L.).

REFERENCES

- Barsony, M. 1989, PhD Thesis, Caltech
 Bender, R., & Möllenhoff, C. 1987, *A&A*, 177, 71
 Boroson, T. A. & Thompson, I. B. 1987, *AJ*, 93, 33
 Caon, N., Capaccioli, M. & D'Onofrio, M. 1994, *A&AS*, 126, 199
 Carlberg, R. G. 1984, *ApJ*, 286, 403
 Canterna, R. 1976, *AJ*, 81, 228
 Cohen, J. G. 1986, *AJ*, 92, 1039
 Davies, R. L., Sadler, E. M., & Peletier, R. F. 1993, *MNRAS*, 262, 650
 Davis, R., & Birkinshaw, M. 1988, *ApJS*, 68, 409
 deVaucouleurs, G., deVaucouleurs, A., Corwin, Jr., H. G., Buta, R. J., Paturel, G. & Fouque, P. 1991, *Third Reference Catalogue of Bright Galaxies*, Springer-Verlag
 Elias, J. 1994, *NOAO Newsletter*, No. 37, 1
 Ferrarese, L., van den Bosch, F. C., Ford, H. C., Jaffe, W. & O'Connell, R. W. 1994, *AJ*, 108, 1598
 Forbes, D. A., Brodie, J. P. & Grillmair, C. J. 1997, *AJ*, 113, 1652
 Franx, M., Illingworth, G., & Heckman, T. 1989, *ApJ*, 344, 613
 Geisler, D. & Forte, J. C. 1990, *ApJ*, 350, L5
 Geisler, D. 1996, *AJ*, 111, 480
 Geisler, D., Lee, M. G. & Kim, E. 1996, *AJ*, 111, 1529
 Jaffe, W., Ford, H. C., O'Connell, R. W., van den Bosch, F. C. & Ferrarese, L. 1994, *AJ*, 108, 1567
 Kent, S. M. 1985, *PASP*, 97, 165
 King, I. R. 1966, *AJ*, 71, 64
 King, I. R. 1978, *AJ*, 221, 1
 Kormendy, J., & Djordovski, S. 1989, *ARA&A*, 27, 235
 Larson, R. B. 1975, *MNRAS*, 173, 671
 Lauer, T. R. 1985, *ApJS*, 57, 473
 Lee, M. G., Kim, E. & Geisler, D. 1998, *AJ*, 115, 947
 McLaughlin, D. E. 1999, *AJ*, 117, 2398
 Michard, R. 1985, *A&AS*, 59, 205
 Mihalas, D., & Binney, J. 1981, *Galactic Astronomy* (W.H Freeman and Company, San Francisco), 309
 Peletier, R. F., Davis, R. L., Illingworth, G. D., Davis, L. E. & Cawson, M. 1990, *AJ*, 100, 1091
 Pilachowski, C., Goodrich, B., Binkert, B. & Africano, J. 1989, *NOAO Newsletter*, No. 15, 14
 Taylor, B. J. 1985, *ApJS*, 60, 577
 Tift, W. G. 1969, *AJ*, 74, 354
 Vader, J. P., Vigroux, L., Lachièze-Rey, M., & Souviron, J. 1988, *A&A*, 203, 217
 van den Bosch, F. C., Ferrarese, L., Jaffe, W., Ford, H. C. & O'Connell, R. W. 1994, *AJ*, 108, 1579
 White, S. D. M. 1980, *MNRAS*, 191, 1p